SAND96-2467C

SAND--96-2467C

CHARACTERISTICS OF SELF-SENSING ACTUATION FOR ACTIVE CONTROL

CONF-970233--6

RECEIVED NOV 06 1996 OSTI

Pat Barney*, Jim Redmond*, David Smith+

* Senior Members Technical Staff
Experimental Structural Dynamics Dept.
P.O. Box 5800 MS 0557
Sandia National Laboratories
Albuquerque, NM 87185-0557

\+ Graduate Research Assistant
Machine Tool Research Center
Mechanical Engineering Dept.
University of Florida
Gainesville, FL 32611

ABSTRACT

The benefits of a collocated sensor actuator pair are well known within the controls community. Generally speaking, collocation offers the use of simple control algorithms with reduced instabilities due to spillover. One method for achieving collocation is the implementation of a "sentuator" in which a piezoelectric element functions simultaneously as both a sensor and an actuator. Past work in utilizing a sentuator has primarily been limited to piezoelectric films and patches mounted to flexible structures. Additional papers have provided information and methodology for dealing with the non-linear aspects of a piezoceramic sentuator. The need arises for methods of self-sensing when performing active vibration control of very stiff structures. A method for understanding and using self-sensing lead zirconate titanate stacks for active vibration control is presented. This paper specifically provides a basic understanding of self-sensing methods as applied to stiff structures for the purposes of control. The discussion of the methodology is followed by a simple example in which active vibration control is applied to a model of a boring bar with embedded PZT stacks.

NOMENCLATURE

A, B, C, D	State Space Matrices
C_2	Bridge Capacitance
C_3	Reference Capacitance
C_p	Piezoelectric Capacitance
$\mathcal{D}$	Electric Displacement
E	Electric Field
F_p	Piezoelectric Force
L	Stack Length
ΔL	Change in Stack Length
S	Strain
T	Stress
V	Voltage Across Stack
V_c	Control Voltage Applied to Bridge
V_e	Piezoceramic Excitation Voltage
V_o	Bridge Voltage
V_p	Strain Induced Voltage
a	Cross Sectional Area
c^E	Elastic Modulus
c_s	Damping Coefficient
d_{33}, e	Piezoelectric Constants
k_p	Stack Stiffness
k_s	Structural Stiffness
m	Mass
n	Number of Wafers in Stack
q_c	Applied Charge
q_p	Strain Induced Charge
x	Displacement
$\underline{y}$	State Vector
α^2	Stack to Structure Stiffness Ratio
β	Nondimensional Frequency of Excitation
γ	Bridge Capacitance Ratio
ε^S	Permittivity at Constant Strain
μ	Reference Capacitance Ratio
ω	Frequency of Excitation
ω_p	Stack Frequency
ω_s	Structural Natural Frequency

1. INTRODUCTION

Collocated sensors and actuators for structural control have long been recognized for their favorable stability characteristics. Low order, robust feedback algorithms can be implemented to efficiently damp vibrations while minimizing the potential for destabilizing spillover. However, the realization of a truly collocated actuator/ sensor pair has proven difficult to achieve, since slight differences between sensor and actuator locations can have destabilizing effects on higher modes. High order global control methodologies that tolerate noncollocation have subsequently been developed, but the possibility of achieving robust stability without sacrificing controller simplicity has nourished a strong interest in collocated control.

Recent developments using a single piezoelectric element as both sensor and actuator have offered new hope in the quest for collocation. Early work combined

DISTRIBUTION OF THIS DOCUMENT IS UNLIMITED

MASTER

DISCLAIMER

Portions of this document may be illegible in electronic image products. Images are produced from the best available original document.

DISCLAIMER

This report was prepared as an account of work sponsored by an agency of the United States Government. Neither the United States Government nor any agency thereof, nor any of their employees, make any warranty, express or implied, or assumes any legal liability or responsibility for the accuracy, completeness, or usefulness of any information, apparatus, product, or process disclosed, or represents that its use would not infringe privately owned rights. Reference herein to any specific commercial product, process, or service by trade name, trademark, manufacturer, or otherwise does not necessarily constitute or imply its endorsement, recommendation, or favoring by the United States Government or any agency thereof. The views and opinions of authors expressed herein do not necessarily state or reflect those of the United States Government or any agency thereof.

piezoelectric elements with passive electrical networks to augment structural damping [1]. This concept was expanded to the case of active vibration control using a self-sensing actuator, or "sentuator," and demonstrated on a flexible cantilevered beam fitted with a piezoceramic patch [2]. This development hinted at the potential for contamination of the sensor signal resulting from bleed-through of the excitation voltage. The sensitivity of the sensor signal to critical components of the sentuator circuitry was subsequently examined in detail [3]. This work indicated that closed-loop performance in some cases can be improved by tuning the bleed-through to influence open loop pole-zero spacing. The difficulty of hand tuning the circuit components to match the nonlinear and environmentally dependent properties of the sentuator has fueled interest in the development of adaptive compensation techniques to eliminate feed-through of the excitation voltage to the sensor signal [4].

This paper focuses on the implementation of a lead zirconate titanate (PZT) stack as a sentuator for collocated control. In particular, the issue of sensor signal contamination resulting from excitation feed-through is examined for applications in which the host structure is much stiffer than the piezoceramic element. This work is motivated by manufacturing problems for which integrated stack actuators have been used to actively damp bending vibrations in thick bars and plates [5-6]. The following section describes the electro-mechanical properties of a piezoelectric stack, leading to its implementation as a sentuator. A single degree of freedom example with a low stack to structure stiffness ratio is presented to illustrate the influence of excitation feed-through on the open loop transfer function. In section 3, an open loop transfer function measured on a cantilevered boring bar fitted with a PZT stack sentuator for controlling bending vibrations is presented. Despite efforts to minimize sensor contamination, the data exhibits significant feed-through of the excitation voltage. A simulated control example featuring partial feed-through compensation coupled with integral feedback is then presented, followed by a summary of results and a brief description of ongoing experimental investigations in section 4.

2. THE PZT STACK SENTUATOR

2.1 The PZT Transducer

Figure 1 provides the mechanical and electrical models of a PZT stack. In the electrical model depicted, a control voltage V_e is applied to the stack with an internal capacitance denoted C_p. The small effects of the internal resistance are neglected, and V_p is the internally generated voltage due to strain on the stack. In the mechanical model shown, the stress T is a function of the electrical field applied and the actuator strain. Consequently, the resultant stack extension depends on the applied voltage and on the stiffnesses of the stack and host structure. This fundamental electro-mechanical coupling of a piezoelectric device can be summarized as [2]

$$T = c^E S + eE \quad (1)$$

$$\mathcal{D} = eS + \varepsilon^S E \quad (2)$$

in which c^E is the elastic modulus measured at constant field, S is the strain, e is the piezoelectric coefficient, E is the electric field, $\mathcal{D}$ is the electric displacement, and ε^S is the permittivity measured at constant strain.

Equations 1 and 2 are normally presented in tensor notation to reflect the multiple degrees of freedom available in a piezoelectric material, but for the purposes of this paper, only the one dimensional PZT stack relationships need be considered. In addition, equations (1) and (2) do not reflect the nonlinear aspects which are inherent to all piezoelectric materials. Although methods for treating non-ideal behavior of the piezoceramic such as hysteresis and nonlinear dielectric constants are being developed [4], they will not be considered in this paper.

To aid understanding of the coupling, a simplified model is given in Figure 2 which shows a piezoceramic stack reacting to external mechanical and electrical stimuli. Figure 2a shows the stack functioning as a pure sensor in which an external force induces a strain in the material, resulting in an electric displacement. Figure 2b shows the element reacting to an applied field. Since the actuator is unconstrained, it expands freely resulting in zero stress. The same field is applied to the

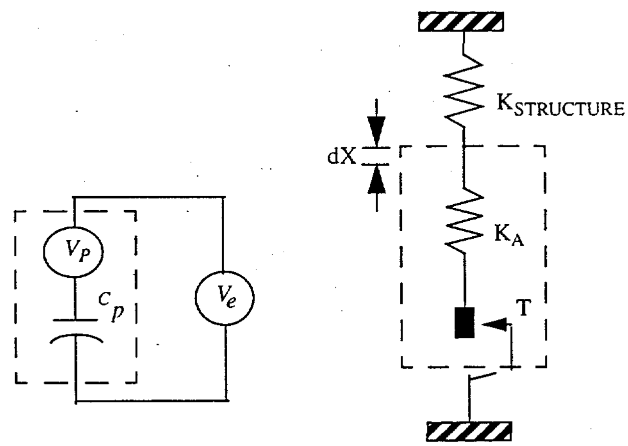

A) Electrical Model *B)* Mechanical Model

Figure 1. - Electrical and Mechanical Model of a PZT Stack Actuator/Sensor.

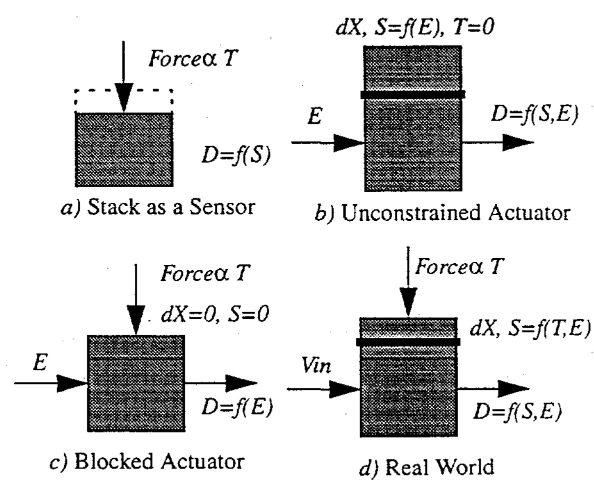

Figure 2. - Operational Modes of a One-Dimensional Piezoceramic Stack.

element with blocked boundary conditions in Figure 2c. Here the actuator does not expand, resulting in zero strain and maximum stress. Most realistic applications are depicted in Figure 2d, in which the boundary conditions possess some flexibility. In this case, the electric displacement is a function of both the applied field and the strain, making it suitable as both a sensor and an actuator.

The use of a piezoelectric stack as a sentuator requires further understanding of the voltage that is produced as a consequence of deformation. For a stack mounted in a compliant structure, the voltage across the stack can be expressed as

$$V = \frac{1}{C_p}(q_c - q_p) \tag{3}$$

in which q_c is the charge due to excitation and q_p is the charge resulting from the strain. Examining only the strain component of the voltage, a more amenable expression can be obtained by noting that

$$q_p = a d_{33} c^E S \tag{4}$$

in which a is the cross-sectional area of the stack, and d_{33} is the more common piezoelectric coefficient. Substituting in $S = \Delta L/L$ and recognizing $(ac^E)/L$ as axial stiffness, the strain induced voltage is given by

$$V_p = \frac{k_p d_{33}}{C_p}\Delta L \tag{5}$$

in which k_p is the axial stiffness of the stack.

2.2 The Sentuator Bridge

Since strain induces a charge on piezoelectric elements, a bridge network can be assembled to extract the voltage internally produced while removing the effects of the excitation voltage. The common method for extraction is the bridge arrangement shown in Figure 3, which shows the piezoelectric stack linked to a reference capacitor C_3, and two bridge capacitors C_2. This particular bridge arrangement will result in a self-sensing strain output; replacing the two bridge capacitors with resistors will result in the rate of strain as the output [2]. For the strain sensing bridge circuit, the differential output voltage V_o can be expressed in the Laplace domain as

$$V_o(s) = \frac{C_p}{C_2 + C_p} V_p(s) + \left[\frac{C_p}{C_2 + C_p} - \frac{C_3}{C_2 + C_3}\right] V_c(s) \tag{6}$$

which exhibits both a component due to strain and a feed-through component of the excitation voltage. A simpler expression is obtained by dividing through by the stack capacitance and simplifying the feed-through component to yield

$$V_o(s) = \frac{1}{\gamma + 1} V_p(s) + \left[\frac{\gamma(1-\mu)}{(\gamma+1)(\gamma+\mu)}\right] V_c(s) \tag{7}$$

where the capacitance ratios are given by $\gamma = C_2/C_p$, and $\mu = C_3/C_p$.

To obtain a well balanced bridge, the reference capacitor should be matched to the actuator capacitance, and the bridge capacitors should be matched to each other. Assuming that the capacitances are well matched, the measured differential voltage will be proportional to the strain induced voltage, and no excitation voltage will contaminate the sensor signal. However, because the stack capacitance depends on the strain, electric field, and frequency, it is difficult to maintain balance in practice. The sensitivity of the bridge output to reference capacitor mismatch depends in part on the stack to host structure stiffness ratio. This matter will be explored further in the following section.

2.4 Bridge Voltage Sensitivity

The importance of the feed-through term in the self sensing bridge cannot be overlooked, since an exact capacitance match throughout the frequency range of interest is difficult to achieve in practice. This problem is further exacerbated by applications in which the actuator stiffness is small in comparison to the inherent stiffness of the structure. To illustrate, we consider the use of a piezoelectric stack as both sensor and actuator in the mass spring system shown in Figure 4. The piezoelectric stack is mounted in parallel to the structural stiffness k_s and damping c_s elements, consistent with the intended application of controlling bending vibrations in thick bars and plates. As previously indicated, the force generated by the

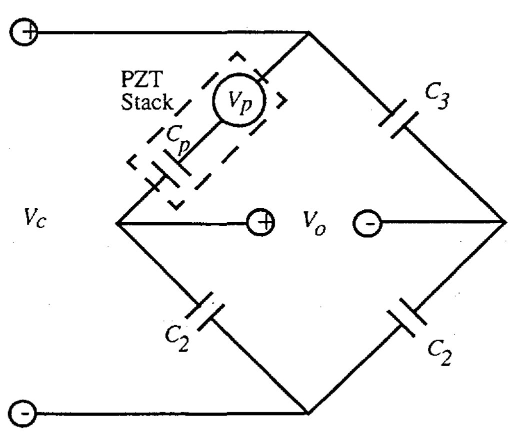

Figure 3. - Self Sensing Actuator Bridge Based on Reference 1.

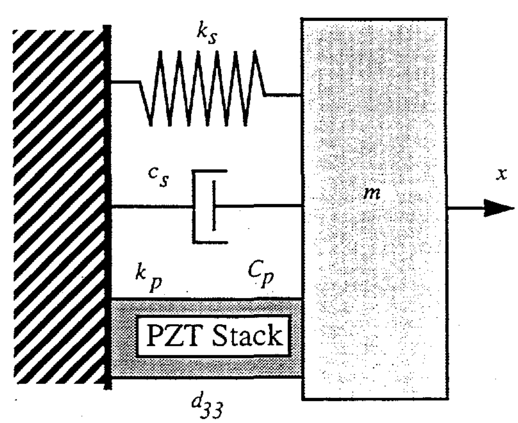

Figure 4. - Single Degree of Freedom System with PZT Stack Sentuator.

piezoelectric stack depends both on the input voltage and the actuator deformation according to

$$F_p(t) = k_p(nd_{33}V_c(t) - x(t)) \quad (8)$$

where n denotes the number of wafers in the stack. In equation 8, the passive damping contribution of the actuator resulting from the material loss factor is assumed small in comparison to c_s. Also, the effect of the actuator mass relative to the structural mass is assumed small. The stack force drives the mass-spring system with the displacement to input voltage transfer function written as

$$\frac{x(s)}{V_c(s)} = nd_{33}\left[\frac{\omega_p^2}{s^2 + 2\zeta\omega_s s + \omega_s^2 + \omega_p^2}\right]. \quad (9)$$

Here, the piezoelectric and structural natural frequencies are defined as $\omega_p^2 = k_p/m$, and $\omega_s^2 = k_s/m$, respectively. Note that the overall stiffness of the system is enhanced by the passive stiffening effects of the stack.

In addition to the excitation offered by the input voltage, the stack generates a charge proportional to the strain. The strain induced voltage to input voltage transfer function in the frequency domain is readily obtained by setting $s = j\omega$ and substituting equation 5 into equation 9 to yield

$$\frac{V_p(j\omega)}{V_c(j\omega)} = \frac{nd_{33}^2k_p}{C_p}\left[\frac{\omega_p^2}{(\omega_s^2 + \omega_p^2 - \omega^2) + 2\zeta\omega_s\omega j}\right] \quad (10)$$

A simpler expression is obtained by dividing through by the host structure's natural frequency,

$$\frac{V_p(j\beta)}{V_c(j\beta)} = \frac{nd_{33}^2k_p}{C_p}\left[\frac{\alpha^2}{1 + \alpha^2 - \beta^2 + 2\zeta\beta j}\right] \quad (11)$$

in which $\alpha^2 = k_p/k_s$ is the stack to structure stiffness ratio and $\beta = \omega/\omega_s$ is the dimensionless frequency of excitation.

Since the strain induced charge cannot be directly measured, it must be inferred by the output of the sentuator bridge described in section 2.2. Substituting equation 11 into equation 7 and rearranging gives

$$\frac{V_o(j\beta)}{V_c(j\beta)} = \frac{1}{\gamma+1}\left\{\frac{nd_{33}^2k_p}{C_p}\left[\frac{\alpha^2}{1 + \alpha^2 - \beta^2 + 2\zeta\beta j}\right] + \frac{\gamma(1-\mu)}{(\gamma+\mu)}\right\} \quad (12)$$

which is the nondimensional frequency transfer function relating bridge output to stack excitation voltage for the single degree of freedom structure.

In the absence of feed-through ($\mu = 1$), equation 12 provides a true representation of strain. However, the nonlinear character of the stack capacitance makes it difficult to realize a perfect capacitance match for all operating conditions. Furthermore, the feed-through term is more prominent when the actuator is mounted in a relatively stiff structure ($\alpha^2 << 1$). To illustrate, we let $\gamma = 1$ and set the stack to structure stiffness ratio to be $\alpha^2 = 0.03$. This is consistent with the structural parameters of the boring bar example of the following section. With the remaining coefficients describing the stack parameters set equal to unity, three transfer functions with varying degrees of feed-through are shown in Figure 5. With a perfect capacitance match, no zeros are evident in the transfer function. However, as μ is decreased, a zero approaches the pole from infinity, resting at $\beta = 1.25$ with a 90% match. Conversely, as μ is increased, the zero wraps around to the frequency regime below the pole location, and is located at $\beta = 0.64$ when C_3 is equal to $1.1C_p$. As a consequence of the low stack to structure stiffness ratio, the zero location is extremely sensitive to mismatch between the reference capacitor and the piezoelectric stack. For even moderate levels of mismatch, close pole-zero spacing can result, compromising the effectiveness of feedback control. One approach to solving this dilemma is to use feed through compensation. An example illustrating this technique is described in the following section.

3. SENTUATOR CONTROL OF A BORING BAR

3.1 Open Loop System

The problem of excitation feed-through for the sentuator is especially problematic for applications in which the structure is much stiffer than the stack. An example of this is the boring bar experiment shown in Figure 6. The benefits of active vibration control in boring operations have recently been demonstrated [7] using active dampers. The experiment shown differs from previous work in that integrated piezoelectric stack actuators induce bending moments in the bar to counter lateral vibrations. A Kennametal model A32DDUNR4 2 inch diameter boring bar was modified to accept four Physique Instrumente Model P840.1 piezoelectric stacks in pockets near the bar root. The 16 inch long bar was mounted in a four jawed chuck leaving an effective tool length of 12 inches. Mounted at 90 degree intervals, the two stacks influence bending vibrations in each of two orthogonal axes through creation of axial forces offset from the bar's neutral axis. The pocket dimensions were nominally 2 inches in length, 0.6 inches wide, and 0.45 inches deep. Pocket depths were minimized to maintain structural integrity and to avoid interference with the bar's centrally located

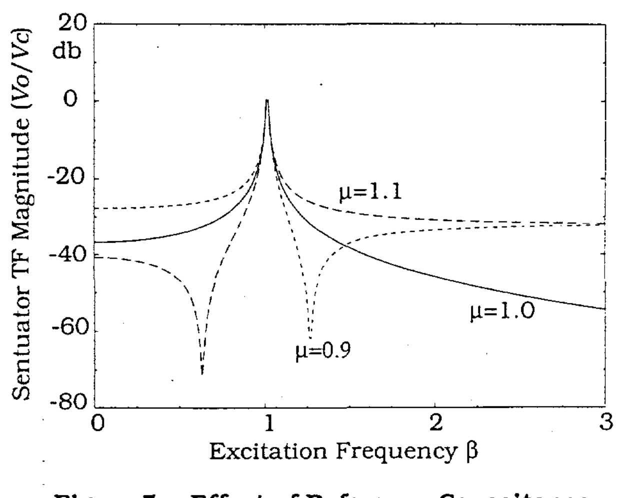

Figure 5. - Effect of Reference Capacitance Mismatch on Sentuator Transfer Function for Single Degree of Freedom System with 3% Actuator Stiffness Ratio.

0.25 inch diameter coolant tunnel. To avoid the transmission of bending stresses to the fragile PZT stacks, the stack/bar interfaces feature single point contacts with both mechanical and electrical preloads holding the stacks in place. Contact points were located at 0.5 inches and 2.5 inches as measured from the chuck jaws with a radial offset distance of 0.84 inches. A complete description of the actuation methodology is given in [5].

For this example, the inclusion of the actuator sets increases the lateral stiffness of the boring bar an estimated 3% in both the X and Y directions. Individually, the actuator/structure stiffness ratio is approximately 1.5%, so a significant feed-through component was expected with the implementation of the sentuator circuitry. One sentuator transfer function measured along the X direction is shown in Figure 7, which includes the effects of signal amplification. The transfer function resembles that of a load cell indicating

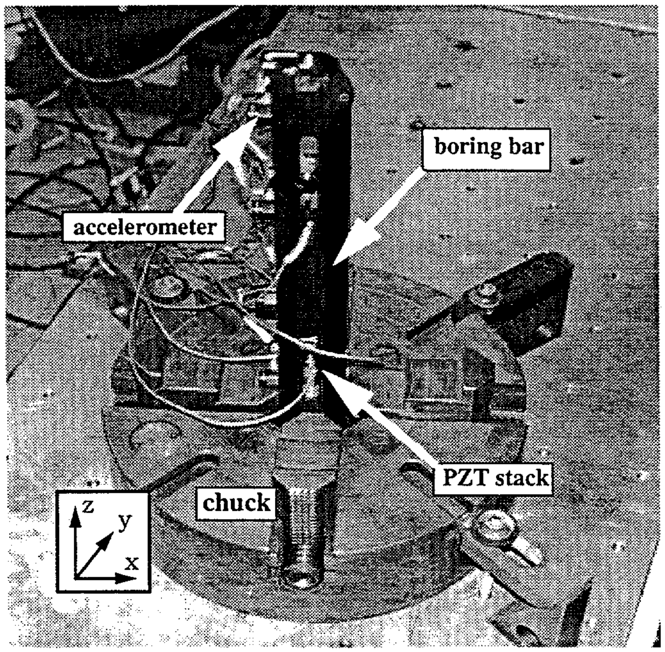

Figure 6. - Active Boring Bar Testbed with Integrated PZT Stack Sentuator Mounted at Bar Root.

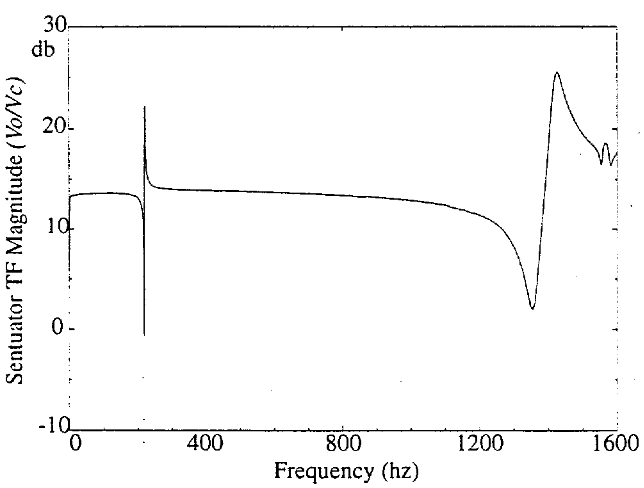

Figure 7. - Measured Open Loop Transfer Function for Boring Bar Sentuator.

that a strong feed-through component was present despite using the same model stack as the reference capacitor. The resultant zero-pole pattern makes it difficult to augment the damping in the first mode near 220 hz through the implementation of simple feedback control algorithms. As previously described, feed-through compensation can be used to increase pole-zero spacing, making the active control more effective.

3.2 Simulated Integral Feedback Control

Using the Eigensystem Realization Algorithm [8], a fourth-order model of the form

$$\dot{\underline{y}}(t) = A\underline{y}(t) + BV_c(t) \tag{13}$$

$$V_o(t) = C\underline{y}(t) + DV_c(t) \tag{14}$$

was fit to the experimental sentuator transfer function. This model formed the basis of a dynamic simulation used to investigate the feasibility of active control for improving first mode damping. A feedback circuit showing partial feed-through compensation combined with integral-like feedback is given in Figure 8. Integral feedback has previously been demonstrated for control of space structures using active struts featuring piezoelectric stack actuators and load cell sensors [9]. The open and closed loop model transfer functions shown in Figure 9 reveal that an increase in the zero-pole spacing was achieved as a consequence of the feed-through compensation. Furthermore, the integral feedback increased the damping in the first mode from 0.2% to 5.1%, and from 1.3%to 6.9% in the second mode. Figure 10 compares the open and closed loop

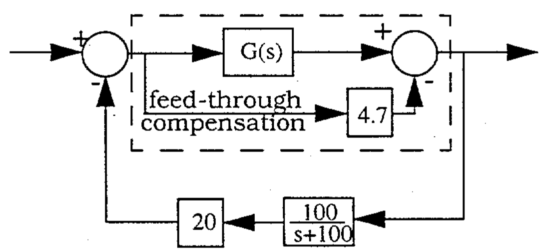

Figure 8. - Closed Loop System for Integral Feedback Control of the Active Boring Bar.

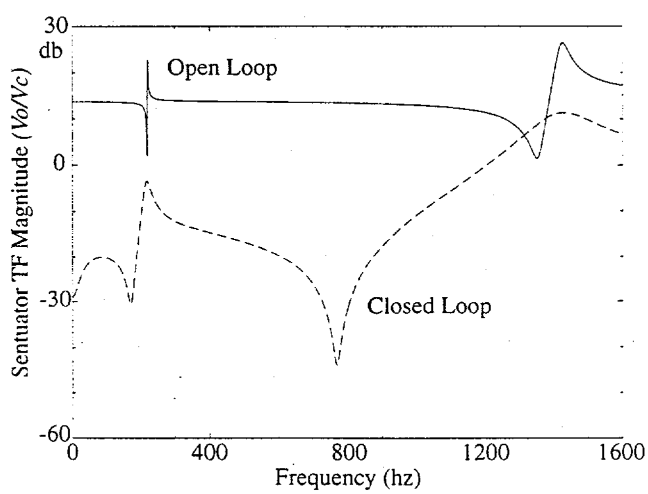

Figure 9. - Open and Closed Loop Transfer Function Magnitudes for the Model of the Active Boring Bar with PZT Stack Sentuator.

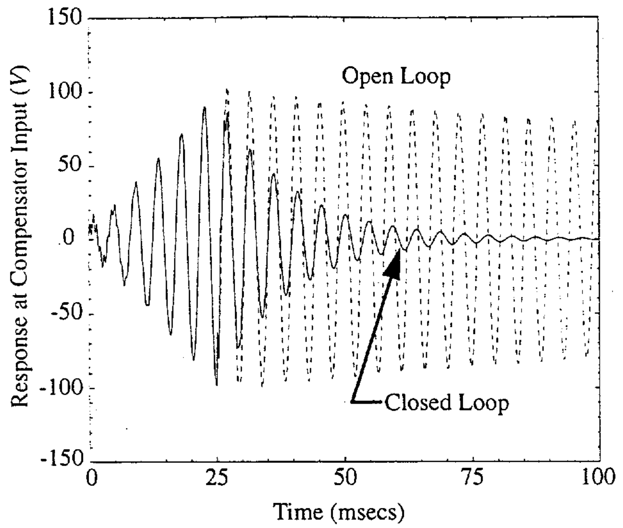

Figure 10. - Simulated Open and closed Loop Responses for Ring-Down Tests.

responses to a ring down test. In this simulated test, the system was excited by the sentuator with a 40 V amplitude sine wave at the first natural frequency for 0.025 seconds. For the controlled case, the loop was then closed at the completion of the excitation cycle and the vibration was significantly diminished by 0.1 seconds. For the uncontrolled case, the vibration continued well beyond the time window.

4. SUMMARY

This paper explored the implications of using the piezoelectric sentuator concept on relatively stiff structures. In particular, sensor signal contamination by the excitation voltage resulting from capacitance mismatches was found to be especially problematic for applications with low sentuator to structure stiffness ratios. Such problems have recently been encountered in the manufacturing arena, in which PZT stacks were used to control bending vibrations in thick bars and plates. An example transfer function taken from a boring bar application exhibited a high degree of contamination, indicating that many such applications can benefit from feed-through compensation techniques. A simulated example featuring constant feed-through compensation coupled with integral feedback yielded significant improvements to first and second mode damping. Future work will focus on experimental verification of these concepts, and the implementation of more sophisticated nonlinear, frequency dependent compensation techniques.

5. ACKNOWLEDGEMENTS

The authors wish to thank Eric Anderson of CSA and Jeff Dohner of Sandia for their valuable suggestions. This work was performed at Sandia National Laboratories, which is operated for the U.S. Department of Energy under Contract No. DE-AC04-94AL85000.

6. REFERENCES

[1] Hagood, N.W. and von Flotow, A.H., Damping of Structural Vibrations with Piezoelectric Materials and PAssive Electrical Networks," Journal of Sound and Vibration, Vol. 146, No. 2, pp. 243-268, 1991.

[2] Dosch, J.J., Inman, D.J., and Garcia, E., "A Self Sensing Piezoelectric Actuator for Collocated Control," *Journal of Intelligent Material Systems and Structures*, Vol. 3, pp. 167-185, 1992.

[3] Anderson, E.H., and Hagood, N.W., "Simultaneous Piezoelectric Sensing/Actuation: analysis and Application to Controlled Structures," *Journal of sound and Vibration*, Vol. 174, No. 5, pp. 617-639, 1994.

[4] Vipperman, J.S., and Clark, R.L., "Complex Adaptive Compensation of Nonlinear Piezoelectric Sensoriactuators," *Proceedings of the AIAA Adaptive Structures Forum*, AIAA-96-1266-CP, pp. 1-11, 1996.

[5] Redmond, J.M., Parker, G.G., Barney, P.S., and Rodeman, R., "Active Control of Bending Vibrations in Thick Bars Using PZT Stack Actuators," Proceedings of the ASME Dynamic Systems and Control Division, Vol. 2, pp. 831-835.

[6] Redmond, J., Barney, P., "Active Vibration Control of a Photolithography Platen for Increased Resolution and Throughput," Proceedings of the 37th AIAA Structures, Structural Dynamics, and Materials Conference, pp. 1190-1197, 1996.

[7] Tewani, S.G., Rouch, K.E., and Walcott, B.L., "A Study of Cutting Process Stability of a Boring Bar with Active Dynamic Absorber," International Journal of Machine Tools, Vol. 35, No. 1, pp. 91-108, 1995.

[8] Dohner, J.L., "System Identification for Robust Control Design," Sandia Report, SAND95-0843, April 1975.

[9] Preumont, A., Dufour, J.P., and Malekian, C., "Active Damping by a Local Force Feedback with Piezoelectric Actuators," *Journal of Guidance, Control, and Dynamics*, Vol. 15, No. 2, pp. 390-395, 1992.